Initial Oxidation and Interfacial Diffusion of Zn on Faceted MgO(111) Films

ARTICLE *in* LANGMUIR · JULY 2008

Impact Factor: 4.46 · DOI: 10.1021/la801314s · Source: PubMed

4 AUTHORS:

Ming-shan Xue
Nanchang Hangkong University
54 PUBLICATIONS **425** CITATIONS
SEE PROFILE

Qinlin Guo
Chinese Academy of Sciences
63 PUBLICATIONS **856** CITATIONS
SEE PROFILE

Kehui Wu
Chinese Academy of Sciences
101 PUBLICATIONS **1,951** CITATIONS
SEE PROFILE

Jiandong Guo
Chinese Academy of Sciences
63 PUBLICATIONS **605** CITATIONS
SEE PROFILE

Initial Oxidation and Interfacial Diffusion of Zn on Faceted MgO(111) Films

Mingshan Xue, Qinlin Guo,* Kehui Wu, and Jiandong Guo

Beijing National Laboratory for Condensed Matter Physics, Institute of Physics, Chinese Academy of Sciences, P. O. Box 603, Beijing 100190, China

Received April 28, 2008. Revised Manuscript Received June 9, 2008

The interaction of zinc and faceted MgO(111) thin films prepared on a Mo(110) substrate was investigated in situ by using various surface analysis techniques, including X-ray photoelectron spectroscopy, ultraviolet photoelectron spectroscopy, Auger electron spectroscopy, high-resolution electron energy loss spectroscopy, and low-energy electron diffraction. The results revealed that three-dimensional Zn islands exist on the faceted MgO(111) films and that no chemical interaction takes place at the interface at room temperature. Initially, deposited Zn is stable at temperatures below 400 K and diffuses into MgO at temperatures above 425 K. A portion of Zn is oxidized at $\sim 10^{-6}$ mbar O_2 at room temperature. An interfacial phase of $Zn_xMg_{1-x}O$ was formed after Zn was exposed to $\sim 10^{-6}$ mbar O_2 at temperatures ≥ 500 K. The faceted structure on the MgO(111) surface is of a disadvantage for the epitaxial growth of ZnO films.

Introduction

Metal-oxide systems have received considerable interest due to their wide applications in many fields, such as microelectronics, gas sensors, photovoltaic devices, and catalysts.[1−3] Interfacial properties referring to interfacial diffusion, surface chemistry, charge transfer, hybridization, and so on in metal-oxide systems play crucial roles in determining their applications.[3,4] Among oxides, single crystal MgO and its ordered thin films, owing to their simple structure (rock-salt), are considered to be one of the most suitable templates for fundamental studies on metal-oxide systems. Through those studies, more detailed information on interfacial interactions (i.e., initial nucleation and growth, interfacial chemistry, and physics) can be collected.

Because of potential applications of ZnO in blue light-emitting and ultraviolet optoelectronic devices,[5,6] scientists have attempted to prepare high-quality ZnO with optical properties by various techniques (e.g., molecular beam epitaxy and pulsed laser deposition). Although success in the preparation of ZnO single crystals on a sapphire (0001) surface by using a buffer layer of MgO(111) was achieved, some fundamental problems, such as the growth mechanism, formation of defects, and band gap engineering, are far from being solved.[7,8] The insertion of MgO(111) layers between ZnO and Al_2O_3 can reduce the surface energy and defect density and increase the nucleation sites of ZnO. However, the (111) face of MgO is a polar and unstable surface, and it easily diverges into facets with {100} planes on its surface to decrease its surface free energy. Even for a cleaved MgO(111) crystal, the MgO(111) surface has polar instability and easily is covered by a series of trigonal pyramids characterized by three sets of {100} facets (consisting of (100), (010), and (001) faces) inclined by 54.7° to the original surface normal.[9] The formation of {100} facets is in qualitative agreement with theories of the stability of ionic crystal surfaces based on the Madelung potential and lattice dynamics calculations.[10,11] Experimentally, however, more information on their interfacial physics and chemistry is lacking. Considering the difficulty in preparing ideal MgO(111) films due to polar instability,[4] in view of fundamental research, it is necessary to investigate the interfacial interaction between Zn and faceted MgO, which will be helpful for further understanding the mechanism of high-quality ZnO growth.

In this paper, we report in detail the initial growth, oxidation, and interfacial diffusion of Zn on faceted MgO(111) thin films prepared on a Mo(110) substrate. The experiments were performed in situ under ultrahigh vacuum (UHV) conditions by means of X-ray photoelectron spectroscopy (XPS), ultraviolet photoelectron spectroscopy (UPS), Auger electron spectroscopy (AES), high-resolution electron energy loss spectroscopy (HREELS), and low-energy electron diffraction (LEED). The results revealed that 3-D Zn islands were formed on the faceted MgO(111) films and that no interfacial interaction was found at room temperature (RT). Initially deposited Zn is stable at temperatures below 400 K and partially diffuses into MgO layers at >425 K. An interfacial phase of $Zn_xMg_{1-x}O$ was observed after exposing Zn to $\sim 10^{-6}$ mbar O_2 at ≥ 500 K.

Experimental Procedures

The experiments were carried out in two systems: ESCALAB-5 (VG Scientific Ltd.) and ELS-22 (Leybold-Heraeus GmbH) with base pressure of 8×10^{-10} and 2×10^{-10} mbar, respectively. The former is equipped with reverse-view optics for LEED, dual-anode X-ray sources (Mg and Al), and a He I ($h\nu = 21.2$ eV) source for XPS and UPS, respectively. The latter consists of AES, HREELS, and LEED. In XPS measurements, the Mg Kα X-ray source ($h\nu =$ 1253.6 eV) with a pass energy of 50 eV was used. The binding energy (BE) was calibrated with respect to pure bulk Au $4f_{7/2}$ (BE = 84.0 eV) and Ag $3d_{5/2}$ (BE = 368.3 eV) lines, and the accuracy of measured BE was better than 0.15 eV. In the HREELS

* Corresponding author. E-mail: qlguo@aphy.iphy.ac.cn.

(1) Henry, C. R. *Surf. Sci. Rep.* **1998**, *31*, 231.
(2) Campbell, C. T. *Surf. Sci. Rep.* **1997**, *27*, 1.
(3) Fu, Q.; Wagner, T. *Surf. Sci. Rep.* **2007**, *62*, 431.
(4) Gajdardziska-Josiforska, M.; Plass, R.; Schofield, M. A.; Schofield, M. A.; Giese, D. R.; Sharma, R. J. *J. Electron Microsc.* **2002**, *51*, 13.
(5) Chen, Y.; Ko, H.; Hong, S.; Yao, T. *Appl. Phys. Lett.* **2000**, *76*, 559.
(6) Ozgur, U.; Alivov, Y. I.; Teke, A.; Reshchikov, M. A.; Dogan, S.; Avrutin, V.; Cho, S.-J.; Morkoc, H. *J. Appl. Phys.* **2005**, *98*, 41301.
(7) Zheng, K.; Guo, Q.; Xue, M.; Guo, D.; Liu, S.; Wang, E. G. *Thin Solid Films* **2007**, *515*, 7167.
(8) Thornton, G.; Crook, S.; Chang, Z. *Surf. Sci.* **1998**, *415*, 122.
(9) Henrich, V. E. *Surf. Sci.* **1976**, *57*, 385.
(10) Srinivasan, R.; Lakshmi, G. *Surf. Sci.* **1974**, *43*, 617.
(11) Mark, P. *J. Phys. Chem. Solids* **1968**, *29*, 689.

10.1021/la801314s CCC: $40.75
Published on Web 07/15/2008

measurements, the primary energy of the electron beam was 5.0 eV with a typical resolution of 12−13 meV obtained by the full width at half-maximum (fwhm) height of the elastic peak from the MgO films.

A Mo(110) substrate (10 mm diameter disk, 1.0 mm thick) was spot welded with a Ta filament around its edge, allowing electron bombardment heating to temperatures >2000 K. A C-type thermocouple (W-5% Re/W-26% Re) was spot welded to the edge of the sample for temperature measurements. The Mo(110) surface was treated by annealing at ∼1200 K in $\sim 10^{-7}$ mbar oxygen to remove surface contaminators (mainly C), followed by a subsequent flash to 1500 K without oxygen until no impurities were detected by XPS or AES and a sharp (1 × 1) LEED pattern was observed.

The magnesium and zinc sources were made of pure magnesium ribbon (purity >99.9%) and zinc wire (purity >99.995%) wrapped tightly around a tungsten wire, respectively. Before growth, the two sources were thoroughly degassed by thermal treatment. The deposition rates of Mg and Zn were ∼0.15 and 0.05 ML/min, respectively, calibrated via the intensity ratios of Mg 2p/Mo 3d and Zn 2p/Mo 3d as a function of deposition time by XPS in the ESCALAB-5 chamber and monitored by a quartz crystal oscillator in an ELS-22 chamber.[12] Owing to the 3-D nucleation of Zn, we prefer to use the monolayer equivalent (MLE) to scale the coverage of Zn (for Zn(0001), 1 MLE = 4.33×10^{14} atoms/cm^2).

The MgO thin films with a 10−15 MLE thickness were epitaxially grown on the Mo(110) substrate by evaporating Mg in $\sim 10^{-6}$ mbar O_2 at 673 K, followed by annealing at 800 K in $\sim 10^{-7}$ mbar O_2. As a result, from LEED observations, the spots were split, and some diffusing spots appeared in nonradical directions with the slightly changed primary energy E_p, being characteristic of facets with {100} planes on a polar (111) face, which coincides with a previous study.[13] Then, as-grown faceted MgO(111) films were used as the support for the deposition of Zn. All data were collected at RT.

Results and Discussion

Growth and Morphology of Zn. Figure 1a,b shows the XP spectra of Zn 2p and O 1s core-levels with an increase of Zn coverage step-by-step, respectively. With increasing Zn coverage from 0.1 to 5 MLE, the BE of Zn $2p_{3/2}$ line shifted from 1022.5 to 1021.7 eV. In fact, the BE of Zn $2p_{3/2}$ already shifted to 1021.7 eV at 3 MLE coverage as shown in Figure 1a, characterizing metallic Zn. Note that the BE value at initial deposition (0.1 MLE) is 0.8 eV higher than that from bulk Zn. However, at 0.1−5 MLE, the O 1s line shifts from 531.2 to 531.4 eV, a 0.2 eV difference in BE (Figure 1b). The intensity of the O 1s line changes little even at a coverage of 5 MLE of Zn (Figure 1b). This indicates that the MgO surface is not fully covered by Zn, implying the existence of 3-D islands of Zn on the MgO surface. In addition, no LEED pattern was observed after Zn deposition, indicating the formation of disordered Zn islands.

To identify the chemical information at the interface, the Auger parameter, $\alpha = E_K(\text{Zn LMM}) + E_B(\text{Zn } 2p_{3/2})$, is of much help.[12,14] Here, E_K is the kinetic energy (KE) of the most intense Auger transitions, and E_B is the BE of the most intense core-level photoemission peak in XPS measurements. For Zn^0 and Zn^{2+}, the α values are ∼2014 and 2010 eV, respectively.[15] In the present experiment, the α values we measured ranged from 2013.7 to 2014 eV for all coverages from 0.1 to 5 MLE, characterizing the Zn^0 state. This suggests that a very weak chemical interaction occurred at the Zn-MgO interface at RT. As for the BE shift of 0.8 eV for the Zn 2p line shown in Figure 1a, it may originate from size effects. The BE shift of ∼1 eV to a higher value with decreasing size due to the final state relaxation from bulk metal to small particles/clusters was observed.[3,12,16,17]

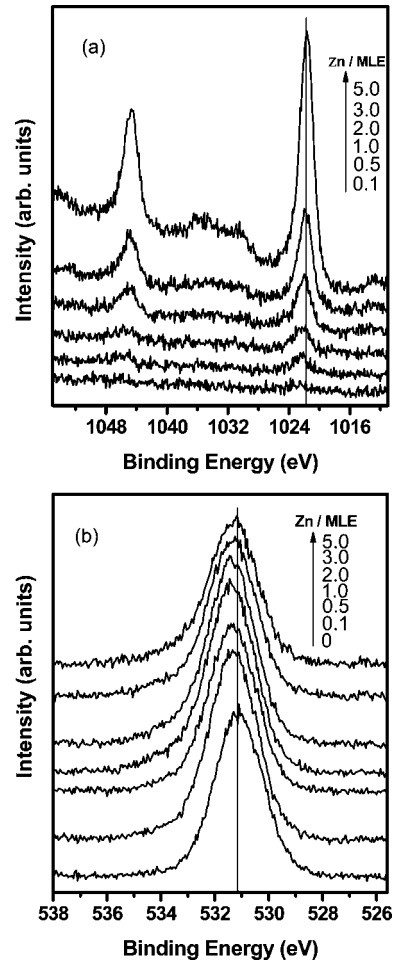

Figure 1. XP spectra of (a) Zn 2p and (b) O 1s core-levels with different coverages of Zn. The vertical lines indicate the BE positions of metallic Zn $2p_{3/2}$ (1021.7 eV) and O 1s (531.2 eV) in MgO, respectively.

Thermal Stability of Zn. To check the thermal stability of Zn on the MgO surface, the sample with 5 MLE of Zn was step-by-step heated from RT to 700 K. The XPS results are shown in Figure 2. With increasing temperature, the intensity of the Zn 2p line gradually decreases. The inset in Figure 2 shows the change of the intensity ratio of Zn $2p_{3/2}$ to O 1s lines as a function of temperature. One can see that the intensity of the Zn 2p line obviously decreases at 400−425 K, suggesting a low adhesion energy of Zn on the MgO surface. Because of the high vapor pressure of metallic Zn, the formation of clusters on the MgO surface further decreases its adhesion ability, and therefore, it results in a rapid decrease of the intensity of the Zn 2p lines. However, their intensities are not changed from 425 to 700 K. As compared to the BE of Zn $2p_{3/2}$ lines at 400 K, its BE is higher (1022.8 eV) at 425 K, implying either chemical information or size effects. The α values are 2013.8 and 2010.2 eV at 400 and 425 K, corresponding to metallic and oxidized Zn on the surface, respectively. As we discussed that the α values are almost the same at initial deposition of Zn at 0−5 MLE coverages, this means that the BE shift after heating at 425 K is not caused by

(12) Guo, D.; Guo, Q.; Zheng, K.; Wang, E. G.; Bao, X. *J. Phys. Chem. C* **2007**, *111*, 3981.
(13) Xue, M.; Guo, Q. *J. Chem. Phys.* **2007**, *127*, 54705.
(14) Wagner, C. D.; Gale, L. H.; Raymond, R. H. *Anal. Chem.* **1979**, *51*, 466.
(15) Moulder, J. F.; Stickle, W. F.; Sobol, P. E.; Bomben, K. D. *Handbook of X-ray Photoelectron Spectroscopy*; Chastain, J., Ed.; PerkinElmer: Eden Prairie, MN, 1992.
(16) Luo, K.; Lai, X.; Yi, C.-W.; Davis, K. A.; Gath, K. K.; Goodman, D. W. *J. Phys. Chem. B* **2005**, *109*, 4064.
(17) Luo, K.; St. Clair, T. P.; Lai, X.; Goodman, D. W *J. Phys. Chem. B* **2000**, *104*, 3050.

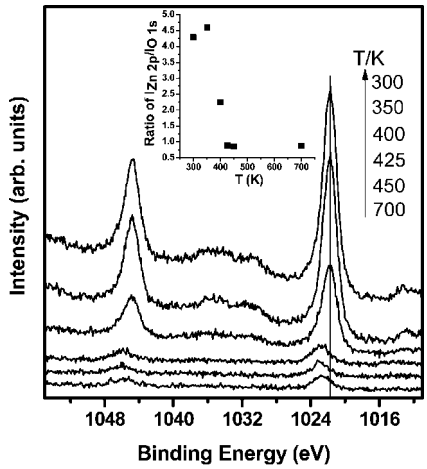

Figure 2. XP spectra of Zn 2p core-level as a function of annealing temperature. Inset shows the evolution of the ratio of the intensity of Zn $2p_{3/2}$ to O 1s lines with an increase of annealing temperature.

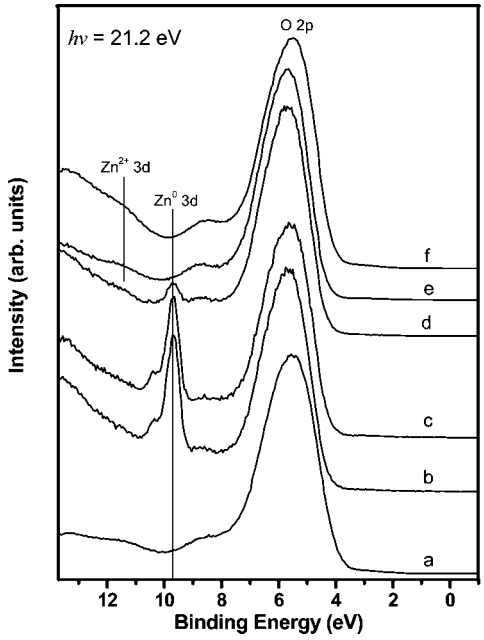

Figure 3. UP spectra (a) for a clean faceted MgO(111) thin film and with 5 MLE Zn at (b) 300 K, (c) 350 K, (d) 400 K, (e) 425 K, and (f) 700 K, respectively.

size effects. Therefore, we conclude that Zn is partially oxidized by surface lattice O at >400 K.

Figure 3 is the UP spectra with different temperature. The spectrum for a clean faceted MgO film is shown in Figure 3a. After depositing Zn on the MgO film at RT, a peak appearing at 9.7 eV is attributed to the Zn 3d line as seen in Figure 3b, indicating a metallic Zn, Zn^0 state. After the sample was heated to 350 K (Figure 3c), the intensity of Zn 3d was the same as that at RT. However, at 400 K (Figure 3d), the intensity of the Zn signal decreased rapidly, and no signal of Zn^0 was detected at 425 and 700 K, as shown in Figure 3e,f. We conclude that, based on the intensity changes of the Zn 3d line in UP spectra, the desorption of Zn on the MgO surface begins at temperatures around 350−400 K.

One interesting result is that no signal of Zn^0 from UP spectra can be detected at ≥425 K, which seems to conflict with the XPS results shown in Figure 2. Since UPS is more sensitive for surface analysis, we should have seen a filled Zn 3d state at 10.5 eV if

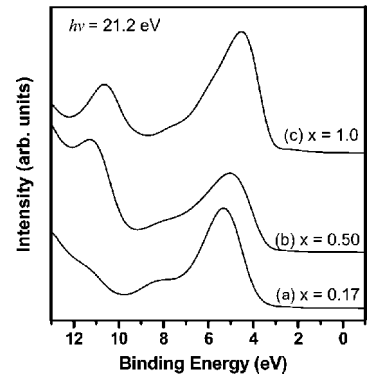

Figure 4. UP spectra of $Zn_xMg_{1-x}O$ thin films with different Zn contents. The films were prepared by codeposition of Zn and Mg in $\sim 10^{-6}$ mbar O_2 at RT, followed by annealing at 600 K for 10 min.

Zn was oxidized to ZnO.[18] Because of a higher incident photon energy (1253.6 eV) and emissive electronic kinetic energy (231 eV for Zn $2p_{3/2}$) in XPS than in UPS (no more than 21.2 eV), XPS gives more information from the subsurface (0.3−7 nm analysis depth). Considering that part of Zn was oxidized at 425 K and kept stable below 700 K, as well as the different detected depths in XPS and UPS measurements, the results indicate an interfacial diffusion of Zn (i.e., part of Zn diffuses into the MgO film).

Because the ionic radius of Zn^{2+} (0.60 Å) is very close to that of Mg^{2+} (0.57 Å), substitution of Zn for Mg in either wurtzite or rock-salt structure without distorting their original structure is allowed.[19,20] In addition, from the UP spectra at 425 and 700 K, a very weak signal around 11−12 eV was observed (marked Zn^{2+} in Figure 3), which was not caused by Zn or ZnO but most likely indicative of the existence of $Zn_xMg_{1-x}O$ due to a high mobility of Zn atoms.[21] The possible formation mechanism of $Zn_xMg_{1-x}O$ is that the Zn atoms occupied the defect sites of Mg or partly substituted for Mg atoms.

To prove the existence of $Zn_xMg_{1-x}O$ layers, we prepared films of $Zn_xMg_{1-x}O$ by codeposition of Zn and Mg in $\sim 10^{-6}$ mbar oxygen for comparison. Figure 4 gives the UP spectra of $Zn_xMg_{1-x}O$ with different x values. Here, the x values were calculated by combining the peak-to-peak intensity with their relative atom sensitivity factors using AES or XPS.[7] For a clean MgO surface (see Figure 3a), the UPS spectrum is in good agreement with a previous study.[22] For a sample with $x = 0.17$ (Figure 4a), a very weak and broad peak around 10.5−12 eV is quite close to the peaks marked Zn^{2+} in Figure 3e,f. With further increasing x to 0.5 and 1, the BE of this peak shifted to 11.3 and 10.6 eV, respectively (Figure 4b,c), and their intensities apparently became strong, indicating a Zn^{2+} state. Note that the BE value is shifted higher while x is decreased. According to the phase diagram, the solid solubility of ZnO in MgO can reach a maximum of 56 atom %.[20] Similar phenomena were found in the Zn/MnO_2 and Pt/SiO_2 systems, in which the metal diffuses into oxide layers to form ternary compounds.[23,24] The results from XPS and α

(18) Girard, R. T.; Tjernberg, O.; Chiaia, G.; Soderholm, S.; Karlsson, U. O.; Wigren, C.; Nylen, H.; Lindau, I. *Surf. Sci.* **1997**, *373*, 409.
(19) Chen, N. B.; Sui, C. H. *Mater. Sci. Eng., B* **2006**, *126*, 16.
(20) Sharma, A. K.; Narayan, J.; Muth, J. F.; Teng, C. W.; Jin, C.; Kvit, A.; Kolbas, R. M.; Holland, O. W. *Appl. Phys. Lett.* **1999**, *75*, 3327.
(21) Tomlins, G. W.; Routbort, J. L.; Mason, T. O. *J. Appl. Phys.* **2000**, *87*, 117.
(22) Yu, Y.; Guo, Q.; Liu, S.; Wang, E. G. *Phys. Rev. B: Condens. Matter Mater. Phys.* **2003**, *68*, 115414.
(23) Garcia, M. A.; Ruiz-Gonzalez, M. L.; Quesada, A.; Costa-Kramer, J. L.; Fernandez, J. F.; Khatib, S. J.; Wennberg, A.; Caballero, A. C.; Martin-Gonzalez, M. S.; Villegas, M.; Villegas, M.; Briones, F.; Gonzalez-Calbet, J. M.; Hernando, A. *Phys. Rev. Lett.* **2005**, *94*, 217206.

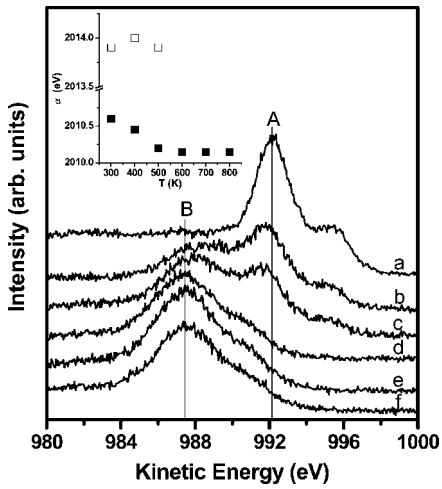

Figure 5. XP spectra of Zn LMM Auger lines from a sample with 3 MLE Zn at RT (a) and after exposure in $\sim 10^{-6}$ mbar O_2 at (b) 300 K, (c) 400 K, (d) 500 K, (e) 600 K, and (d) 700 K, respectively. The vertical lines A and B represent the peak position of LMM Auger lines of metallic and oxidized Zn, respectively. The inset gives the evolution of α as a function of temperature.

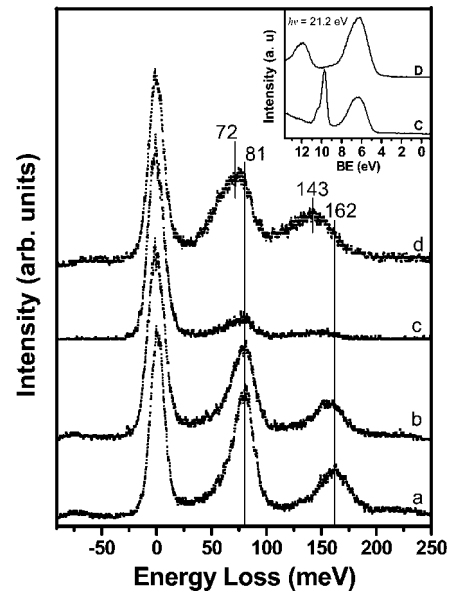

Figure 6. HREEL spectra of (a) clean MgO(111) film, (b) 1 MLE Zn, (c) 5 MLE Zn, and (d) after exposure of Zn to $\sim 10^{-6}$ mbar oxygen by gradually increasing the sample temperature from RT to 500 K. Inset gives the corresponding UP spectra of panels c and d.

measurements indicate that the Zn^{2+} signal exists after 425−700 K, which is not caused by ZnO since the peak of Zn 3d at 9.8 eV was not observed from UPS. Therefore, the appearance of a weak peak around 11−12 eV in Figure 3e,f along with that in Figure 4a suggests the formation of a thin layer of $Zn_xMg_{1-x}O$ (i.e., part of Zn is diffused into MgO to form $Zn_xMg_{1-x}O$ layers). To obtain more information concerning the detailed chemical composition of the film, an angle resolved measurement is expected.

Oxidation of Zn. For Zn, the changes of Auger line and α are dramatic with changes in chemistry, and these changes in chemical states are more distinct than the BE changes for the corresponding core-level lines in XPS measurements. The KE difference between Zn^{2+} and Zn^0 is up to 3.6−4.4 eV in the Zn LMM Auger line but only 0.2−0.6 eV in BE in the Zn $2p_{3/2}$ line.[15] Figure 5 shows the change of Zn LMM Auger line as a function of temperature in $\sim 10^{-6}$ mbar O_2. The XPS result for a sample with 3 MLE of Zn before exposure in O_2 is given in Figure 5a. The peak at 992.1 eV in KE (line A) is from Zn LMM, charactering the Zn^0 state. After the sample was exposed to $\sim 10^{-6}$ mbar O_2 for 20 min at RT (Figure 5b), a new peak appeared at 987.5 eV in KE (line B), revealing partial oxidation of Zn and formation of the Zn^{2+} state. When the temperature was increased to 400 K, more Zn oxide was formed (Figure 5c). At higher temperatures (500, 600, and 700 K), the Zn^0 state (the peak at 992 eV) rapidly reduced, and the lines at 987.5 eV had no change in the peak shape and position (curves d−f in Figure 5), indicating that Zn was oxidized completely. The inset in Figure 5 gives the change of α as a function of temperature, from which we can clearly see that at low temperatures (<500 K), metallic and oxidized Zn (α values were around 2014 and 2010 eV) coexist.

Although these phenomena indicate the formation of Zn oxide after oxidization at ≥500 K, no discernible LEED pattern from ZnO was observed, implying that as-prepared ZnO is disordered. However, one interesting result is that after exposure of Zn/MgO in $\sim 10^{-6}$ mbar O_2 at 500 K directly, Zn is desorbed from the MgO surface due to the low adhesion energy. A similar phenomenon was observed in the Zn/Si(100) system, in which a preoxidized ZnO thin layer is beneficial for further oxidation of Zn films at higher temperatures.[25] In our experiments, we found that the best way for complete oxidation of Zn is to expose it to $\sim 10^{-6}$ mbar O_2 at RT, followed by increasing the substrate temperature gradually. Because of the great discrepancy of vapor pressure between metallic Zn and Zn oxide, the initial oxidation of Zn at RT forms an effective shield to prevent the desorption of metallic Zn, and further increasing the substrate temperature prompts its complete oxidation.[25,26]

Figure 6 gives the HREEL spectra for a clean MgO film and Zn deposited on the surface before and after oxidation. For clean MgO (Figure 6a), the loss of a peak at 81 meV is attributed to the excitation of a long wavelength surface optical phonon (Fuchs−Kliewer mode), which is in good agreement with a previous study.[22] After depositing 1 MLE of Zn at RT, its intensity becomes weak without a shift of the peak position (Figure 6b). The signal of lattice vibration from MgO is still detectable after depositing 5 MLE of Zn (Figure 6c). Because of the sensitivity of HREELS to surface species, the loss of a peak from MgO should not be detected if the Zn film was grown layer-by-layer on its surface. Observed phenomena implied that the growth of Zn on faceted MgO(111) films followed a 3-D model rather than a layer-by-layer model. This result is coincident with that in XPS measurements discussed previously. Besides the low adhesion energy of Zn on MgO, a larger lattice mismatch between MgO and Zn (a = 4.21 Å and d_{O-O} = 2.98 Å for MgO(111) and a = 2.665 Å for Zn(0001)) also can cause the 3-D growth of Zn.[25]

After Zn was oxidized in $\sim 10^{-6}$ mbar oxygen by gradually increasing the substrate temperature from RT to 500 K, a broader loss peak at 72 meV and its second multiple loss peak at 143 meV were observed (Figure 6d). As was reported, the main loss peak from the ZnO crystal was at 68 meV.[27] Since a broader loss feature was located at the range between the main loss peak of ZnO (68 meV) and the main loss peak of MgO (81 meV), the formation of $Zn_xMg_{1-x}O$ is strongly suggested. The inset in Figure

(24) Keck, K.-E.; Kasemo, B. *Surf. Sci.* **1986**, *167*, 313.
(25) Chen, S. J.; Liu, Y. C.; Ma, J. G.; Zhao, D. X.; Zhi, Z. Z.; Lu, Y. M.; Zhang, J. Y.; Shen, D. Z.; Fan, X. W. *J. Cryst. Growth* **2002**, *240*, 467.
(26) Gupta, R. K.; Shridhar, N.; Katiyar, M. *Mater. Sci. Semicond. Process.* **2002**, *5*, 11.
(27) Ibach, H. *Phys. Rev. Lett.* **1970**, *24*, 1416.

6 shows the UP spectra from 5 MLE Zn and after oxidation at 500 K. It clearly indicates that the BE of the Zn 3d core-level shifts from 9.8 to 11.8 eV, corresponding to a transition from Zn^0 to Zn^{2+}.

Practically, MgO(111) can be used as a buffer layer to grow single crystals of ZnO epitaxially on sapphires.[5,6,28] Successful preparation of ZnO/ZnMgO multiple quantum wells indicates the importance of the appearance of the ZnMgO compound.[29,30] An added MgO buffer layer resulting in the formation of a thin $Zn_xMg_{1-x}O$ layer can transitionally reduce the lattice mismatch between ZnO and MgO. This ternary layer may play an important role in the epitaxial growth of ZnO. In present experiments, however, an ordered ZnO film on the faceted MgO(111) surface cannot be obtained by evaporating Zn in oxygen ambience at a substrate temperature from RT to 700 K. Thermodynamically, a {100} facet structure formed on the (111) surface, decreasing the surface free energy of the MgO(111) surface due to the natural character of the polar MgO(111) face, obstructing the epitaxial growth of ZnO. It would be informative to correlate our results with an analysis of the surface morphology using in situ techniques such as tunneling scanning microscopy or atomic force microscopy. However, detailed studies on the ZnMgO interface layer as found in our experiments will be helpful to further understand the growth mechanism of ZnO on a MgO buffer layer.

(28) Setiawan, A.; Ko, H. J.; Hong, S. K.; Chen, Y.; Yao, T. *Thin Solid Films* **2003**, *445*, 213.

(29) Davis, J. A.; Dao, L. V.; Wen, X.; Hannaford, P.; Coleman, V. A.; Tan, H. H.; Jagadish, C.; Koike, K.; Sasa, S.; Inoue, M.; Yano, M. *Appl. Phys. Lett.* **2006**, *89*, 182109.

(30) Gu, X. Q.; Zhu, L. P.; Ye, Z. Z.; He, H. P.; Zhang, Y. Z.; Huang, F.; Qiu, M. X.; Zeng, Y. J.; Liu, F.; Jaeger, W. *Appl. Phys. Lett.* **2007**, *91*, 22103.

Conclusion

By means of in situ various surface analytical techniques, we experimentally investigated the initial growth, oxidation, and diffusion of Zn on faceted MgO(111) thin films. At initial deposition of Zn, the formation of 3-D islands was observed. These islands are unstable, and most of them are desorbed at ~425 K due to the low adhesion energy of Zn on the MgO surface. The Zn islands can be completely oxidized in $\sim 10^{-6}$ mbar O_2 at ≥ 500 K and are stable below 800 K. Diffusion of Zn into MgO to form layers of ternary $Zn_xMg_{1-x}O$ at the interface was observed. The faceted MgO(111) surface is an obstruction to the epitaxial growth of ZnO.

Acknowledgment. We acknowledge the support of this work by the National Science Foundation of China (10574153).

LA801314S